

Research Paper

*These authors contributed equally to this work.

Cite this article: Li P, Li X, Wang W, Tan X, Wang X, Yang X (2021). Transcriptional identification of differentially expressed genes during the prepupal–pupal transition in the oriental armyworm, *Mythimna separata* (Walker) (Lepidoptera: Noctuidae). *Bulletin of Entomological Research* **111**, 485–498. <https://doi.org/10.1017/S0007485321000171>

Received: 16 September 2020
Revised: 28 December 2020
Accepted: 23 February 2021
First published online: 22 March 2021


Keywords:

Gene expression; metamorphosis; *Mythimna separata*; pupation; transcriptome analysis

Author for correspondence:

Xueqing Yang, Email: sling233@hotmail.com;
Xiaoling Tan, Email: tanxiaoling2010@163.com

Transcriptional identification of differentially expressed genes during the prepupal–pupal transition in the oriental armyworm, *Mythimna separata* (Walker) (Lepidoptera: Noctuidae)

Peirong Li^{1,2,*}, Xinru Li^{1,2,*}, Wei Wang^{1,2}, Xiaoling Tan³, Xiaoqi Wang^{1,2}
and Xueqing Yang^{1,2} 

¹College of Plant Protection, Shenyang Agricultural University, Shenyang 110866, Liaoning, China; ²Key Laboratory of Economical and Applied Entomology of Liaoning Province, Shenyang 110866, Liaoning, China and ³State Key Laboratory for Biology of Plant Diseases and Insect Pests, Institute of Plant Protection, Chinese Academy of Agricultural Sciences, Beijing 100193, China

Abstract

The oriental armyworm, *Mythimna separata* (Walker) is a serious pest of agriculture that does particular damage to Gramineae crops in Asia, Europe, and Oceania. Metamorphosis is a key developmental stage in insects, although the genes underlying the metamorphic transition in *M. separata* remain largely unknown. Here, we sequenced the transcriptomes of five stages; mature larvae (ML), wandering (W), and pupation (1, 5, and 10 days after pupation, designated P1, P5, and P10) to identify transition-associated genes. Four libraries were generated, with 22,884, 23,534, 26,643, and 33,238 differentially expressed genes (DEGs) for the ML-vs-W, W-vs-P1, P1-vs-P5, and P5-vs-P10, respectively. Gene ontology enrichment analysis of DEGs showed that genes regulating the biosynthesis of the membrane and integral components of the membrane, which includes the cuticular protein (CP), 20-hydroxyecdysone (20E), and juvenile hormone (JH) biosynthesis, were enriched. Kyoto Encyclopedia of Genes and Genomes (KEGG) pathway analysis indicated that DEGs were enriched in the metabolic pathways. Of these DEGs, thirty CP, seventeen 20E, and seven JH genes were differentially expressed across the developmental stages. For transcriptome validation, ten CP, 20E, and JH-related genes were selected and verified by real-time PCR quantitative. Collectively, our results provided a basis for further studies of the molecular mechanism of metamorphosis in *M. separata*.

Introduction

The oriental armyworm, *Mythimna separata* (Walker) (Lepidoptera: Noctuidae), is typical of widespread migratory pests, and is widely distributed in Asia, Europe, and Oceania (Sharma *et al.*, 2002; Wang *et al.*, 2006; Li *et al.*, 2019a). The agricultural economy suffers giant losses due to damage by *M. separate* of several crops including maize, wheat, and rice (Sharma *et al.*, 2002; Li *et al.*, 2019b). In China, there were about 12 *M. separata* outbreaks in the period 1970–1989 (Ye, 1993); in 2012, the actual losses of grain production caused by *M. separata* were 9.92×10^5 tons, and in 2013, 3.93×10^5 tons (Jiang *et al.*, 2014). Effective control of *M. separata* is essential for the successful harvest of grain (Sharma *et al.*, 2002; Jiang *et al.*, 2014; Li *et al.*, 2019a). At present, the main methods for the control of armyworms are ecological regulation and integrated use of physical, biological, and chemical measures (Jiang *et al.*, 2014). Although these methods are to a degree effective in the control of armyworms, there are significant associated challenges such as insecticide resistance (Li *et al.*, 2019b).

Mythimna separata is a holometabolous insect, and distinguished by the four developmental stages of egg, larva, pupa, and adult (Truman and Riddiford, 1999). The pupal stage is characteristic in Lepidoptera and occurs between vegetative (larval stage) and reproductive growth (adult stage) (Barbora *et al.*, 2011). After *M. separata* larva mature, they drill 1–2 cm into the soil near the roots of host plants and construct a soil chamber for pupation. This transformation is characterized by dramatic morphological and structural changes and is an extremely complicated biological process regulated by an array of genes, hormones, and nutritional components (Dubrovsky, 2004). Manipulation of insect metamorphosis by regulating genes involved in the deformation process has the potential in new pest control strategies.

The epidermis of insects not only protects against pathogens and harmful aspects of the environment but also shapes and maintains activity abilities during normal development (Delon and Payre, 2004; Moussian *et al.*, 2005). Cuticular proteins (CPs) are structural proteins of the insect epidermis. The number of CPs is usually more than 1% of the total insect

coding proteins in the genome (Futahashi *et al.*, 2008), which indicated that CPs may play an important role in growth and development, environmental adaptation, and innate immunity (Andersen *et al.*, 1995; Willis, 2010). The expression of CP genes is closely related to the rhythms of insect molt and metamorphosis (Andersen, 2010). Particularly, morphological characteristics change markedly during prepupal–pupal metamorphosis (Fraenkel and Rudall, 1940; Gu *et al.*, 2013). Guan *et al.* (2006) found that deletion of the epidermal protein gene (*Tweedle D1*) shortens the body of larvae and pupae of *Drosophila melanogaster*, which implicates epidermal protein genes in body formation. In *Anopheles gambiae*, five genes of the CPs family were found to be expressed before the molting of pupae or adults, suggesting that they may be involved in the formation of the outer epidermis of these stages (Togawa *et al.*, 2007). Therefore, CPs are the prime candidates for inclusion in the mechanistic models of insect molting and metamorphosis, and a key to improving the understanding of the biological and physical chemistry, and structural modification that occurs during the development of insects (Shahin *et al.*, 2016).

Juvenile hormone (JH) and 20-hydroxyecdysone (20E) are two major hormones in insects and coordinate in the orchestration of insect growth and development, including features of growth, molting, and reproduction (Liu *et al.*, 2015; Jia *et al.*, 2017). The two hormones appear to complement each other; JH maintains insect growth in larvae, whereas 20E induces metamorphosis of the mature larvae (Truman and Riddiford, 2002; Jindra *et al.*, 2013). JH is synthesized and secreted by insect corpora allata, which regulates the growth of larvae, promotes ovarian maturation, and prevents larvae from entering the next instar stage prematurely (Qu *et al.*, 2018). JH is also involved in the physiological and biochemical processes of the insect body, molting, diapause, and stimulation of the yolk in female adults (Sugahara *et al.*, 2017). 20E is synthesized and secreted by insect prothoracic gland cells. At low concentration, it mainly controls growth, while high concentration mainly regulates the molting between insect larvae and the metamorphosis during development (Nijhout and Callier, 2015). Regulation of metamorphosis by hormones has been studied in many insects, including *Bombyx mori* (Zhang *et al.*, 2017), *Aedes aegypti* (Liu *et al.*, 2018), and *Laodelphax striatellus* (Zhai *et al.*, 2017). From these studies, it appears that JH and 20E co-mediate the prepupal–pupal metamorphosis process of insects by regulating the expression patterns of CPs in various tissues and at various developmental stages.

Previous studies on metamorphosis have been mainly focused on the gene expression patterns of the cytochrome P450s, very high-density lipoproteins, chitinase, chitin deacetylase, serine protease, CPs, and 20E, and which have been studied in insects including *Spodoptera litura* (Gu *et al.*, 2013), *Bactrocera dorsalis* (Chen *et al.*, 2018), *B. mori* (Zhang and Zheng, 2017), and *Helicoverpa armigera* (Zhang *et al.*, 2009; Cai *et al.*, 2016). However, little is known about the molecular mechanisms of metamorphosis in *M. separata*. In this study, we elucidate the larval prepupal–pupal transition by performing a comparative transcriptome analysis. Using RNA-seq, we discovered genes that were differentially expressed at different stages of development, results which were confirmed by real-time quantitative PCR (RT-qPCR). The results of this study provide a foundation for further understanding the molecular mechanism of metamorphosis in *M. separata*, and also open an avenue for establishing RNAi or CRISPR-based pest control through regulating the development of this pest.

Materials and methods

Insects and sample preparation

For these studies, we used a susceptible strain of *M. separata* that has been raised in the laboratory for more than 50 generations without exposure to any insecticides. The feeding method used is described in Li *et al.* (2019b). Mature larvae (ML), wandering stage (W), and three stages of pupation (1, 5, and 10 days after pupation, designated P1, P5, and P10, respectively) were collected (fig. 1). The ML stage of *M. separata* is black or gray black and have the longest body length about 40–50 mm, while the body length of W stage of *M. separata* is shorter than ML and often bent. The P1 are yellow after that the pupae change from yellow to brown. Three biological replicates were conducted, each with three individuals sampled for each developmental stage.

RNA isolation, library construction, and sequencing

We used the Eastep® Super Total RNA Extraction Kit (Promega, Shanghai, China) to extract the total RNA of the whole body of *M. separata* samples, according to the manufacturer's instruction. RNA degradation and contamination were monitored on 1% agarose gels. The concentration and quality of RNA were assessed using a spectrophotometer NanoDrop 2000c (Thermo Fisher Scientific, Waltham, MA, USA).

After total RNA was treated with DNase I, mRNA was enriched with magnetic beads with Oligo (dT). Next, a disruption reagent was added to break the mRNA into short fragments, and we used the disrupted mRNA as a template to synthesize the first-strand cDNA with random hexamers. Next, buffer, dNTPs, and DNA polymerase I were added to synthesize the second-strand cDNA. After purification and recovery, repair of sticky ends, the addition of a base A at the 3' end, and ligation of a sequencing adapter, the resulting fragments were selected for size and enriched by PCR. The constructed library was qualified by the Agilent 2100 Bioanalyzer and ABI StepOnePlus Real-Time PCR System and was sequenced using the Illumina sequencing platform at Shenzhen Hengchuang Gene Technology Co., Ltd. (TGS, Shenzhen, China).

Raw data quality control

The Illumina platform converts sequenced image signals into text signals and stores them in FASTQ format as raw data (Cock *et al.*, 2010). The original sequences were filtered to eliminate low-quality reads. Generally, the accuracy of sequencing decreases with the read length of reads, and reads are considered reliable when the Q20 of Reads is above the set threshold; Q20 indicates that the sequencing error rate is 1%, and Q20 reflects the quality of sequencing. Reads were filtered under the threshold of containing more than 5% N bases, or 50% bases with mass values less than 10. The filtered reads, or clean reads, were used in subsequent analysis.

De novo assembly

The Trinity software (Grabherr *et al.*, 2011) was used to assemble clean reads. Sequences were de-replicated and clustered using Tgicl (Pertea *et al.*, 2003). Unigenes obtained by Tgicl dereplication and splicing are divided into clusters and singletons. In a given cluster, there can be several unigenes (starting with CL, followed by CL family number) with a high degree of similarity

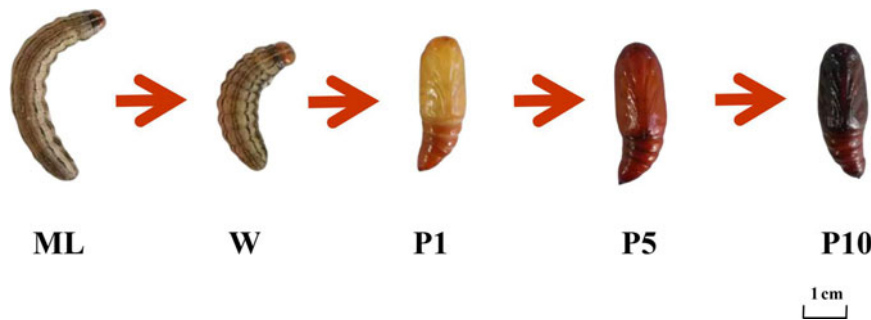


Figure 1. The morphology of five developmental stages including mature larvae (ML), wandering (W), and different stages of pupation (1, 5, and 10 days after pupation were designated P1, P5, and P10) during the pupariation of *M. separata*. (For interpretation of the references to color in this figure legend, the reader is referred to the web version of this article.)

(>70%). Others are singletons (starting with unigene), which are individual unigenes.

Functional annotation of unigene set

The obtained unigene set was annotated by Blast (Altschul *et al.*, 1990) search against several databases: non-redundant nucleic acid sequence (NT), non-redundant protein sequences (NR), Gene Ontology (GO), Clusters of Orthologous Groups of proteins (COG), Kyoto Encyclopedia of Genes and Genomes (KEGG), and manual annotation and expected non-redundant protein database (SwissProt). Blast2GO (Conesa *et al.*, 2005) and NR annotation results were used to annotate the unigene set.

Prediction of the coding sequences of unigenes

According to the functional annotation results, we selected the best-aligned segment as the coding sequences (CDS) of the unigene. The coding sequence was translated into amino acid sequences according to the standard codon table. Unigenes of the un-annotated model were predicted using the CDS predicted in the previous step along with ESTScan (Iseli *et al.*, 1999).

Differential expression analysis of unigenes

RNA-Seq by Expectation-Maximization (Dewey and Li, 2011) was used to calculate the abundance of each transcript for each library. The expression of unigene was standardized by the Fragment Per Kilobase of exon model per Million mapped reads (FPKM) method. Differentially expressed genes (DEGs) between different developmental stages were calculated using the DESeq2 software (Love *et al.*, 2014). The normalization factors were calculated using the trimmed mean of M-values (TMM) method. The threshold false discovery rate (FDR) < 0.05 was adjusted to identify the DEGs by fold change (≥ 2). Significance was adjusted with the threshold FDR < 0.05 and log₂fold change ($|\text{Log}_2\text{FC}| > 1$). Heat maps were drawn in the R programming language. A detailed description of the calculation formula of FPKM and differential expression analysis of unigene is given in the Supplementary Information.

Phylogenetic analysis of DEGs

We constructed a phylogenetic tree to analyze the sequence homology and evolutionary relationships of DEGs of the CPs, 20E, and JH biosynthesis and signaling pathway, including protein sequences from closely related insects *S. litura*, *Athetis dissimilis*, *Trichoplusia ni*, *Spodoptera frugiperda*, *Galleria mellonella*, *B. mori*, *H. armigera*, and *Spodoptera exigua*, which were obtained

from the NCBI repository. Sequences were aligned using Clustalx 1.81. A phylogenetic tree was constructed by MEGA5 with the neighbor-joining method and 1000 bootstrap replicates.

Quantitative real-time PCR

Ten DEGs of the CP genes, and genes in the 20E and JH biosynthesis and signaling pathway, were selected and further verified using quantitative real-time PCR (qRT-PCR). Total RNA of samples from ML, W, P1, P5, and P10 were extracted using RNAiso Plus (Takara, Dalian, China) according to the manufacturer's instructions. The concentration and quality of the extracted RNA were then detected with a NanoDrop 2000c spectrophotometer (Thermo Fisher Scientific). First-strand cDNA was synthesized from 1 μg total RNA using a PrimeScriptTM RT reagent Kit with gDNA Eraser (Takara) according to the manufacturer's instructions. Primer pairs (table S1) were designed using Primer3 (<http://bioinfo.ut.ee/primer3-0.4.0/>). The β -Actin (Accession number: GQ856238) and GAPDH of *M. separata* were used as reference genes (Li *et al.*, 2018; Li *et al.*, 2019b). qRT-PCR was performed on a Bio-Rad CFX96 (BioRad, Hercules, USA) thermal cycler. The relative expression of candidate genes was calculated using the $2^{-\Delta\Delta\text{CT}}$ method (Livak and Schmittgen, 2001). A detailed description of the RT-qPCR is given in the Supplementary Information.

Data analysis

All experiments were performed with three biological replications, and data were analyzed with SPSS Statistics 20 (IBM, Chicago, IL, USA). The differences in mRNA expression in different developmental stages were assessed by one-way analysis of variance and the Duncan-test ($P \leq 0.05$).

Results

Transcriptome sequencing and assembly

Illumina transcriptomes of total RNA were sequenced and assembled for five different developmental stages of *M. separata*. The RNA-seq raw sequence data have been submitted to SRA at NCBI with SRA ID of PRJNA604659 and the accession number SRR11011830. The assembly results totaled 140,562 contigs, with an average length of 1201.07 bp, N50 of 2159 bp, and GC of 41.94%. A detailed description of the assembly results is shown in table 1.

Through Blast search of NCBI (e value < e^{-3}), more than half of genes were annotated (74,059) according to the target sequences. Among them, 6120, 351,851, 47,632, 48,973, 27,817,

Table 1. Statistics derived from the transcriptomes of the prepupal-pupal transition of *M. separata*.

Type	ML			W			P1			P5			P10		
	ML_1	ML_2	ML_3	W_1	W_2	W_3	P1_1	P1_2	P1_3	P5_1	P5_2	P5_3	P10_1	P10_2	P10_3
Read length	150	150	150	150	150	150	150	150	150	150	150	150	150	150	150
Total raw reads	69039382	69164754	67591606	67490458	69128986	69158132	69177054	69114140	72045406	72044646	72046826	72045514	67568700	68120196	67955586
Total raw bases	10305682890	10300653258	10052860508	10058432966	10301743910	10300970632	10299459752	10302286936	10806810900	10806696900	10807023900	10806827100	10054399776	10164894240	10146570656
Total clean reads	68933842	69052290	67486160	67413944	69028242	69076072	69063688	69009642	70819322	70373888	70684470	70499044	67459656	68048264	67876330
Total clean reads ratio (%)	99.85	99.84	99.84	99.89	99.85	99.88	99.84	99.85	98.3	97.68	98.11	97.85	99.84	99.89	99.88
Total clean bases	10289852106	10283784086	10037043740	10046956060	10286632704	10288661722	10282455074	10286612600	10622898300	10556083200	10602670500	10574856600	10038043256	10154104796	10134682664
Total clean bases ratio (%)	99.85	99.84	99.84	99.89	99.85	99.88	99.83	99.85	98.3	97.68	98.11	97.85	99.84	99.89	99.88
Total adapter reads	105540	112464	105446	76514	100744	82060	113366	104498	1224732	1669336	1360734	1545162	109044	71932	79256
Total adapter reads ratio (%)	0.15	0.16	0.16	0.11	0.15	0.12	0.16	0.15	1.7	2.32	1.89	2.14	0.16	0.11	0.12
Total low quality reads	0	0	0	0	0	0	0	0	1352	1422	1622	1308	0	0	0
Total low quality reads ratio (%)	0	0	0	0	0	0	0	0	0	0	0	0	0	0	0
Clean reads GC (%)	49.09	49.32	49.31	48.71	48.02	47.78	50.5	50.75	51.05	47.98	48.28	48.19	49.15	48.97	48.72
Clean reads Q20 (%)	95.43	95.58	95.69	96.6	95.76	95.62	95.37	95.36	93.52	93.79	94.24	93.97	95.55	95.27	95.41
Clean reads Q30 (%)	88.53	88.88	89.15	91.05	89.27	88.97	88.63	88.62	85.72	86.03	86.91	86.39	88.86	88.21	88.5
Detected gene number	77959	78103	80494	84986	82747	83970	85097	84026	83825	84216	84594	84826	81878	82302	81840
Detected SNP number	185569	189935	205222	264546	251061	254948	245617	235817	230275	252275	243880	238048	216526	231909	230538

ML, mature larvae; W, wandering; P1, P5, and P10: 1, 5, and 10 days after pupation. ML_1, ML_2, and ML_3 represent three replicates.

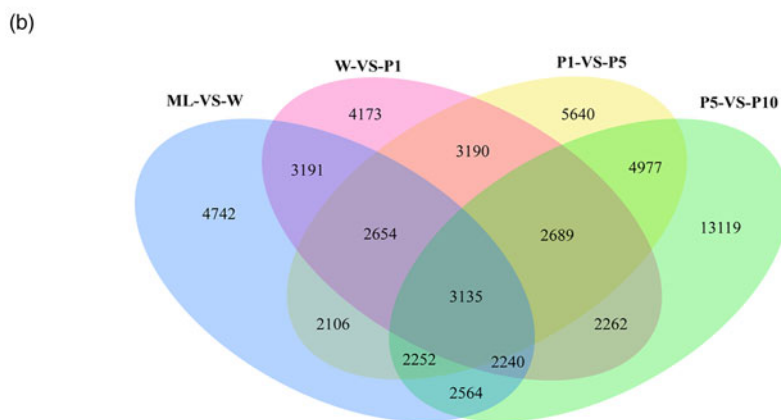
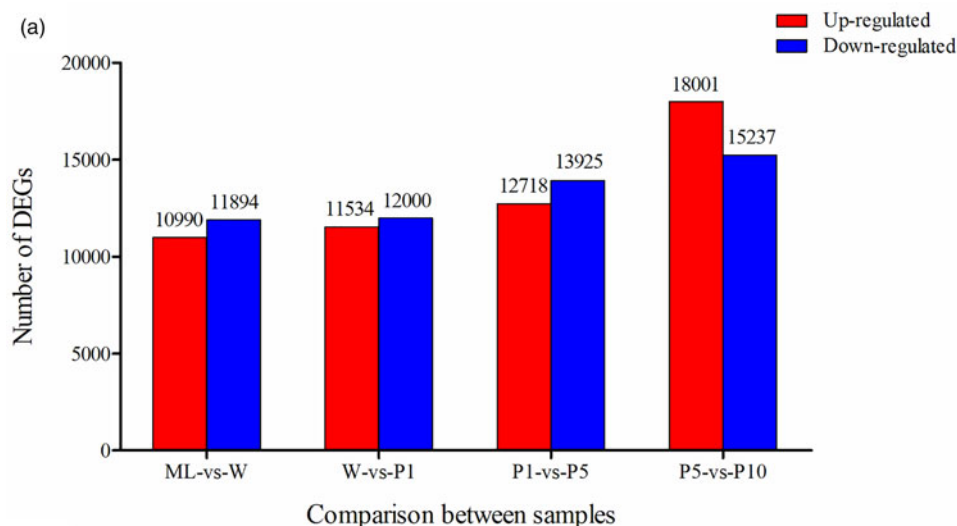


Figure 2. Histogram (a) and Venn diagram (b) analysis of the number of differentially expressed genes (DEGs) between samples. ML, mature larvae; W, wandering; P1, P5, and P10: 1, 5, and 10 days after pupation. (For interpretation of the references to color in this figure legend, the reader is referred to the web version of this article.)

and 31,569 unigenes were annotated in NR, NT, Swiss-Prot, KEGG, COG, and GO, respectively (fig. S1), more than in *B. dorsalis* (Chen *et al.*, 2018) and *Chilo suppressalis* (Sun, 2015). A total of 19,733 unigenes were collectively annotated over the five databases (fig. S2).

Species homology analysis gave the most paired species as *Amyelois transitella* 12,958 (21.17%), *B. mori* 10,635 (17.38%), *Papilio xuthus* 5457 (8.92%), *Papilio machaon* 4205 (6.87%), *Danaus plexippus* 3085 (5.04%), *Operophtera brumata* 2920 (4.77%), *Papilio polytes* 2348 (3.84%), *Plutella xylostella* 2335 (3.82%), *H. armigera* 1148 (1.88%). Other insect species were hit at <1% (fig. S3).

Global analysis of differentially expressed unigenes

There were 22,884 (10,990 up-regulated and 11,894 down-regulated), 23,534 (11,534 up-regulated and 12,000 down-regulated), 26,643 (12,718 up-regulated and 13,925 down-regulated), and 33,238 (18,001 up-regulated and 15,237 down-regulated) DEGs identified between ML and W, W and P1, P1 and P5, and P5 and P10, respectively (fig. 2a). The number of DEGs between other groups is shown in fig. S4. A total of 3135 (0.76%) DEGs were found to be common over the five developmental stages (fig. 2b).

GO distribution analysis of DEGs of the prepupal-pupal transition

GO distribution analysis results showed that these DEGs were categorized into 59 sub-categories belonging to the three main GO categories (biological processes, cellular components, and molecular functions). These categories consisted of 17, 22, and 21 sub-categories respectively (fig. 3).

For biological processes, the oxidation-reduction process was the most significant prepupal-pupal transition-related GO term in ML-vs.-W and P5-vs.-P10, with 700 (6.06%, 193 up-regulated and 507 down-regulated genes) and 1023 (4.77%, 585 up-regulated and 438 down-regulated genes) DEGs, respectively, while the most significant prepupal-pupal transition-related GO term was found in the proteolysis in W-vs.-P1, P1-vs.-P5, with 629 (5.95%, 233 up-regulated and 396 down-regulated genes) and 622 (5.83%, 215 up-regulated and 407 down-regulated genes) DEGs, respectively (fig. 3).

GO enrichment analyses of DEGs showed that the membrane and integral component of the membrane in the cellular component category were significantly enriched. A total of 2388 (8.11%, 1082 up-regulated and 1306 down-regulated genes), 2245 (9.49%, 901 up-regulated and 1344 down-regulated genes), 2404 (9.41%, 1115 up-regulated and 1289 down-regulated genes), and 3615 (8.03%, 2024 up-regulated and 1591 down-regulated genes) DEGs were enriched in the membrane sub-category in

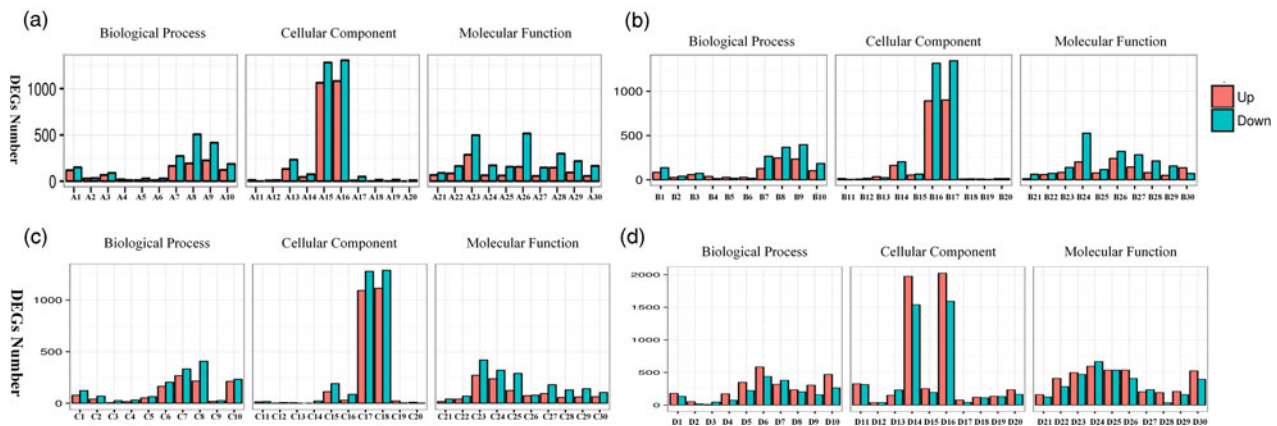


Figure 3. Gene ontology (GO) enrichment analysis of differentially expressed genes (DEGs). (a–d) Represent the GO term for the ML-vs.-W, W-vs.-PP, P1-vs.-P5, and P5-vs.-P10, respectively. Unigene statistical map of ‘up-down’ differential expression of enriched GO term. The x-axis represents the GO term, and the y-axis represents the number of up-down genes corresponding to the GO term. A1–A30 represent the carbohydrate metabolic process, carbohydrate transport, chitin metabolic process, defense response, immune system process, innate immune response, metabolic process, oxidation–reduction process, proteolysis, transmembrane transport, chorion, collagen, extracellular region, extracellular space, integral component of membrane, membrane, mitochondrial inner membrane, mitochondrial membrane, mitochondrial proton-transporting ATP synthase complex, coupling factor F(o), troponin complex, chitin binding, heme binding, hydrolase activity, iron ion binding, monooxygenase activity, oxidoreductase activity, oxidoreductase activity, acting on paired donors, with incorporation or reduction of molecular, peptidase activity, serine-type endopeptidase activity, serine-type peptidase activity GO term, respectively. B1–B30 represent the carbohydrate metabolic process, carbohydrate transport, chitin metabolic process, defense response to bacterium, immune system process, innate immune response, oxidation–reduction process, proteolysis, transmembrane transport, chorion, collagen, cytoskeleton, extracellular region, extracellular space, integral component of membrane, membrane, mitochondrial membrane, mitochondrial proton-transporting ATP synthase complex, coupling factor F(o), peroxisome, carboxylic ester hydrolase activity, chitin binding, heme binding, hydrolase activity, monooxygenase activity, oxidoreductase activity, peptidase activity, serine-type endopeptidase activity, serine-type peptidase activity, structural constituent of cuticle GO term, respectively. C1–C30 represent the carbohydrate metabolic process, defense response, defense response to bacterium, lipid metabolic process, metabolic process, oxidation–reduction process, proteolysis, steroid hormone-mediated signaling pathway, transport, Golgi membrane, Golgi stack, LUBAC complex, chorion, extracellular region, extracellular space, integral component of membrane, membrane, postsynaptic membrane, troponin complex, carboxylic ester hydrolase activity, chitin binding, hydrolase activity, oxidoreductase activity, peptidase activity, sequence-specific DNA binding transcription factor activity, serine-type endopeptidase activity, serine-type peptidase activity, structural constituent of cuticle, transporter activity GO term, respectively. D1–D10 represent the carbohydrate metabolic process, glycolysis, innate immune response, ion transport, metabolic process, oxidation–reduction process, proteolysis, translation, transmembrane transport, transport, cytoplasm, cytosolic large ribosomal subunit, extracellular region, integral component of membrane, intracellular, membrane, mitochondrial inner membrane, mitochondrion, ribonucleoprotein complex, ribosome, calcium ion binding, catalytic activity, hydrolase activity, metal ion binding, nucleotide binding, oxidoreductase activity, peptidase activity, structural constituent of cuticle, structural constituent of ribosome, transferase activity GO term, respectively. (For interpretation of the references to color in this figure legend, the reader is referred to the web version of this article.)

ML-vs.-W, W-vs.-P1, P1-vs.-P5, and P5-vs.-P10, respectively. Integral component of membrane was enriched with 2346 (7.97%, 1064 up-regulated and 1282 down-regulated genes), 2208 (9.33%, 892 up-regulated and 1316 down-regulated genes), 2372 (9.28%, 1093 up-regulated and 1279 down-regulated genes), and 3514 (7.80%, 1975 up-regulated and 1539 down-regulated genes) DEGs in ML-vs.-W, W-vs.-P1, P1-vs.-P5, and P5-vs.-P10, respectively (fig. 3). These DEGs were mainly associated with the solute carrier family, MFS transporter, low-density lipoprotein receptor, glucuronosyltransferase, ATP-binding cassette (ABC), P450, alcohol-forming fatty acyl-CoA reductase, ATPase, NADH dehydrogenase, stearyl-CoA desaturase, chitin, fatty acids, and E3 ubiquitin-protein (table S3). Also, the CPs, 20E, and JH-related genes, which are involved in the metamorphic development of Lepidoptera insects (Willis, 2010; Liu *et al.*, 2015), were also identified in the membrane and integral component of membrane sub-categories (table S4), suggesting these genes are likely to play a role in the prepupal–pupal transition of *M. separata*.

Hydrolase activity was the most significantly affected GO term under molecular function in ML-vs.-W, W-vs.-P1, P1-vs.-P5, with 784 (6.79%, 286 up-regulated and 498 down-regulated genes) and 727 (9.49%, 201 up-regulated and 526 down-regulated genes), 689 (6.46%, 271 up-regulated and 418 down-regulated genes) DEGs, respectively. Metal ion binding was significantly

enriched in P5-vs.-P10, with 1262 (5.88%, 596 up-regulated, and 666 down-regulated genes) (fig. 3).

KEGG pathway analysis of DEGs potentially involved in the prepupal–pupal transition

KEGG pathway analysis indicated that the DEGs were enriched in the metabolic pathways during the prepupal–pupal transition of *M. separata*. These DEGs were mainly associated with starch and sucrose metabolism, pyrimidine metabolism, protein digestion, and absorption (fig. 4). In the metabolic pathways, there were 2218 (16.85%, 745 up-regulated and 1473 down-regulated genes), 2053 (16.26%, 890 up-regulated and 1163 down-regulated genes), 2046 (14.64%, 914 up-regulated and 1132 down-regulated genes), and 3037 (16.14%, 1890 up-regulated and 1147 down-regulated genes) DEGs in ML-vs.-W, W-vs.-P1, P1-vs.-P5, and P5-vs.-P10, respectively.

Besides, there were only 35 (0.27%), 26 (0.21%), 28 (0.20%), and 37 (0.2%) DEGs enriched in insect hormone biosynthesis, which was closely associated with JH and 20E, and 78 (0.59%), 73 (0.58%), 79 (0.57%), 143 (0.76%) and 60 (0.46%), 50 (0.40%), 70 (0.50%), and 73 (0.39%) DEGs enriched in CPs belongs to the GnRH signaling pathway and the ErbB signaling pathway in ML-vs.-W, W-vs.-P1, P1-vs.-P5, and P5-vs.-P10, respectively (fig. S5).

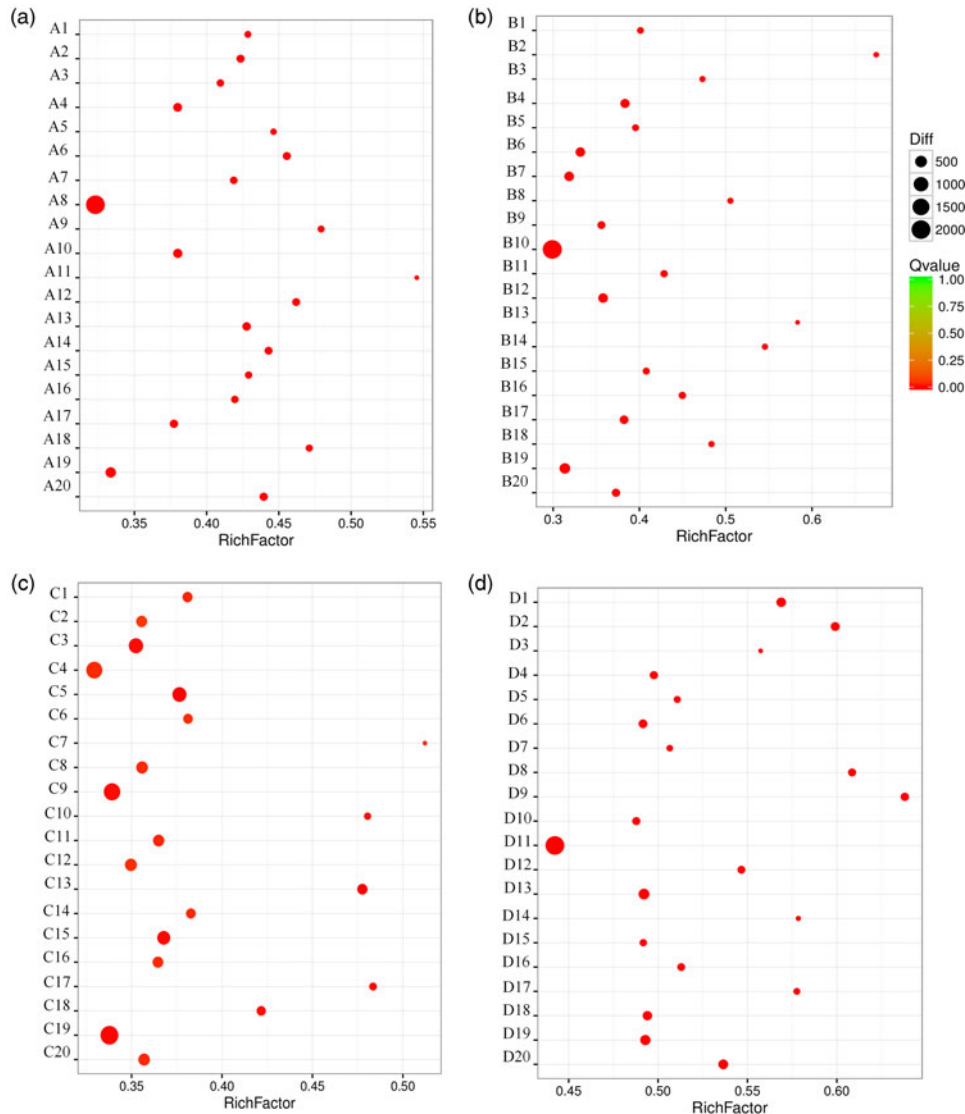


Figure 4. Kyoto Encyclopedia of Genes and Genomes (KEGG) analysis of specific differentially expressed genes (DEGs) in different stages of *M. separata*. (a–d) Represent the KEGG pathway for the ML-vs.-W, W-vs.-PP, P1-vs.-P5, and P5-vs.-P10, respectively. RichFactor indicates the percentage of the ratio of genes in each pathway vs. the total genes in the term. A1–A20 represent steroid hormone biosynthesis, starch and sucrose metabolism, retinol metabolism, protein digestion and absorption, phenylalanine metabolism, pentose and glucuronate interconversions, metabolism of xenobiotics by cytochrome P450, metabolic pathways, malaria, lysosome, glycosaminoglycan degradation, galactose metabolism, ECM–receptor interaction, drug metabolism–other enzymes, drug metabolism–cytochrome P450, chemical carcinogenesis, bile secretion, ascorbate and aldarate metabolism, amoebiasis, amino sugar and nucleotide sugar metabolism KEGG pathway, respectively. B1–B20 represent tyrosine metabolism, riboflavin metabolism, renin-angiotensin system, protein digestion and absorption, phenylalanine metabolism, phagosome, peroxisome, other glycan degradation, neuroactive ligand–receptor interaction, metabolic pathways, malaria, lysosome, glycosphingolipid biosynthesis–ganglio series, glycosaminoglycan degradation, fatty acid elongation, fat digestion and absorption, ECM–receptor interaction, complement and coagulation cascades, amoebiasis, amino sugar and nucleotide sugar metabolism KEGG pathway, respectively. C1–C20 represent steroid hormone biosynthesis, retinol metabolism, RNA polymerase, pyrimidine metabolism, protein digestion and absorption, prion diseases, primary immunodeficiency, pentose and glucuronate interconversions, herpes simplex infection, glycosaminoglycan degradation, galactose metabolism, fatty acid metabolism, fatty acid elongation, fat digestion and absorption, ECM–receptor interaction, dorso-ventral axis formation, complement and coagulation cascades, biosynthesis of unsaturated fatty acids, amoebiasis, ABC transporters KEGG pathway, respectively. D1–D20 represent *Vibrio cholerae* infection, ribosome, renin secretion, RNA polymerase, pyruvate metabolism, phagosome, pathogenic *Escherichia coli* infection, Parkinson’s disease, oxidative phosphorylation, non-alcoholic fatty liver disease (NAFLD), metabolic pathways, hypertrophic cardiomyopathy (HCM), Huntington’s disease, glyoxylate and dicarboxylate metabolism, ECM–receptor interaction, dilated cardiomyopathy, cardiac muscle contraction, carbon metabolism, amoebiasis, Alzheimer’s disease KEGG pathway, respectively. (For interpretation of the references to color in this figure legend, the reader is referred to the web version of this article.)

We further investigated the gene families which were of particular interest as potential targets for the prepupal–pupal transition of *M. separata* below.

The number of DEGs detected in the CPs, 20E, and JH biosynthesis

A total of 30 genes encoding CPs, and 17 and seven genes involved in 20E and JH biosynthesis, respectively, were detected

during the prepupal–pupal transition of *M. separata* (table 2). The number of genes in CPs, 20E, and JH in the five different development stages of *M. separata* is similar (table S5). We tested whether those genes were clustered consistently in a phylogenetic context. Results showed that CP (fig. S6), 20E (fig. S7), and JH (fig. S8) genes from *M. separata* were well clustered into their relevant phylogenetic branches based on the phylogenetic analysis with eight lepidopteran insects including *S. litura*, *A. dissimilis*, *T.ni*, *S. frugiperda*, *G. mellonella*, *B. mori*, *H. armigera*, and *S. exigua*.

Table 2. Differentially expressed genes in the prepupal–pupal transition of *M. separata*

Gene ID	ML-vs.-W	W-vs.-P1	P1-vs.-P5	P5-vs.-P10	Blast nr	Genbank number
<i>Cuticular proteins</i>						
CL9076.Contig3_All	+1.7	–	–1.4	–	Epidermal growth factor receptor isoform X1	MW365961
CL1027.Contig5_All	–	+1.1	–2.8	–1.1	1-phosphatidylinositol 4,5-bisphosphate phosphodiesterase γ -1	MW365962
CL12980.Contig3_All	–	–	–	+1.8	Calcium/calmodulin-dependent protein kinase type II α chain	MW365963
CL16856.Contig2_All	–	+1.4	–1.7	–	Nuclear migration protein nud C	MW365964
Unigene15668_All	–	–	–	–1.1	Nud C domain-containing protein 3	MW365965
CL1779.Contig9_All	+1.7	–	–	–	Protein kinase C, brain isozyme isoform X1	MW365966
CL13841.Contig4_All	–	–	–	–1.4	E3 ubiquitin-protein ligase CBL-B-B isoform X2	MW365967
CL1699.Contig11_All	+1.2	–	–	–	E3 ubiquitin-protein ligase CBL-B-B isoform X2	MW365968
CL3149.Contig3_All	+2.4	–1.2	–1.5	–	TBC1 domain family member 23	MW365969
CL1279.Contig108_All	+3.3	–2.3	–	–	Signal transducer and activator of transcription 5B isoform X2	MW365970
CL1337.Contig49_All	+1.9	–	–	–1.1	Tyrosine-protein kinase Src64B isoform X1	MW365971
CL2288.Contig92_All	–	–	–	–	Tyrosine-protein kinase Src64B isoform X3	MW365972
CL16647.Contig3_All	+1.6	–	–	–	Focal adhesion kinase 1 isoform X1	MW365973
CL4698.Contig2_All	–	–	–	–	Serine/threonine-protein kinase PAK mbt	MW365974
CL7815.Contig1_All	–	–	–	–2.2	Serine/threonine-protein kinase PAK 3	MW365975
CL1585.Contig16_All	+1.7	–1.4	–	–	Acid phosphatase type 7-like	MW365976
CL9103.Contig5_All	–	–	+2	–	Dual specificity mitogen-activated protein kinase 4-like	MW365977
CL4397.Contig3_All	–	–	–	+1.2	Stress-activated protein kinase JNK isoform X1	MW365978
Unigene12087_All	–	–	–	+1.3	Transcription factor jun-D	MW365979
CL18975.Contig2_All	–	–	–1.7	–	SHC-transforming protein 1	MW365980
CL6698.Contig6_All	–	–	–	–	Protein son of sevenless	MW366012
CL2596.Contig51_All	+2.6	–1.6	–	–	GTPaseHRas	MW365981
CL8021.Contig5_All	+1.6	–	–	–	Raf homolog serine/threonine-protein kinase phl isoform X1	MW365982
Unigene8645_All	–	–	–	–	Dual specificity mitogen-activated protein kinase dSOR1 isoform X1	MW365983
CL14604.Contig2_All	–1.8	–1.6	–	–	Gonadotropin-releasing hormone receptor isoform X1	MW365984
CL6175.Contig4_All	–	–1.6	–2	+2.5	Gonadotropin-releasing hormone receptor	MW365985
CL10689.Contig4_All	–	–	–	–1	Guanine nucleotide-binding protein G(q) subunit α isoform X2	MW365986
CL9739.Contig5_All	–	–	–	+2.6	1-phosphatidylinositol 4,5-bisphosphate phosphodiesterase isoform X2	MW365987
CL7899.Contig3_All	–4.9	+4.9	–1.3	–	Putative protein kinase C delta-type homolog isoform X4	MW365988
CL10379.Contig10_All	+2.7	–	–3.8	–	Matrix metalloproteinase-14 isoform X2	MW365989

<i>Juvenile hormone</i>						
CL3825.Contig60_All	-1.4	+3.8	-2.6	+1.4	Farnesol dehydrogenase-like	MW365990
CL5146.Contig76_All	-2	+2.9	-3.3	-	Odorant binding protein 23	MW365991
CL9391.Contig2_All	-	-2.7	-	-2.3	Juvenile hormone acid methyltransferase	MW365992
Unigene19996_All	-	-	-	+3	Juvenile hormone acid O-methyltransferase-like	MW365993
CL16686.Contig3_All	-	+1.8	-1.5	-	Farnesoateepoxidase-like	MW365994
CL15147.Contig1_All	-1.2	-	+2.9	+1.4	Calexcitin-2	MW365995
CL17942.Contig2_All	-6.6	-	-1.3	+2	Calexcitin-2-like	MW365996
Unigene10260_All	-5.9	-	-	-	Sarcoplasmic calcium-binding proteins I, III, and IV-like	MW365997
CL1111.Contig45_All	-4.7	-	-	-	Carboxylesterase	MW366013
CL14984.Contig2_All	-3.5	-	-	-	Carboxylesterase 12	MW365998
CL11190.Contig1_All	+3.9	-3.8	-3.5	-	Juvenile hormone epoxide hydrolase-like	MW365999
CL15275.Contig2_All	-4.9	-	-	-	Juvenile hormone epoxide hydrolase-like	MW366000
CL16665.Contig4_All	-	-1	+2.1	-1.7	Juvenile hormone epoxide hydrolase-like	MW366001
CL18477.Contig4_All	+3	-4.3	-	+3.8	Juvenile hormone epoxide hydrolase-like	MW366002
CL4540.Contig4_All	-2.4	-	-	-2.2	Juvenile hormone epoxide hydrolase-like	MW366003
CL5616.Contig2_All	-	+2.8	-	-	Juvenile hormone epoxide hydrolase-like	MW366004
CL817.Contig4_All	-2.4	-2.2	-1.7	+1.7	Juvenile hormone epoxide hydrolase	MW366005
<i>20-hydroxyecdysone</i>						
CL14010.Contig2_All	-	-	-1.8	-2.2	Cytochrome P450 307A1	MW366006
Unigene18829_All	-	-	-	-	Cytochrome P450 306A1	MW366007
CL8044.Contig1_All	-	-	-	-	Cytochrome P450 CYP339A1	MW366008
Unigene29505_All	-	-	-	-	Cytochrome P450 302A1	MW366014
Unigene4431_All	-	-1.6	-	-	Cytochrome P450 315A1	MW366009
CL17221.Contig1_All	-	-2.4	+2.1	-1.3	Cytochrome P450 314A1	MW366010
CL19241.Contig2_All	-	-	-	-2.2	Cytochrome P450 CYP18A1	MW366011

ML, mature larvae; W, wandering; P1, P5, and P10: 1, 5, and 10 days after pupation.

The second to fifth columns of numbers represent $|\log_2\text{Ratio}|$.

+ is up-regulated, - is down-regulated and - represents no DEGs. Differential gene screening conditions are $\text{FDR} \leq 0.01$ and $|\log_2\text{Ratio}| \geq 1$.

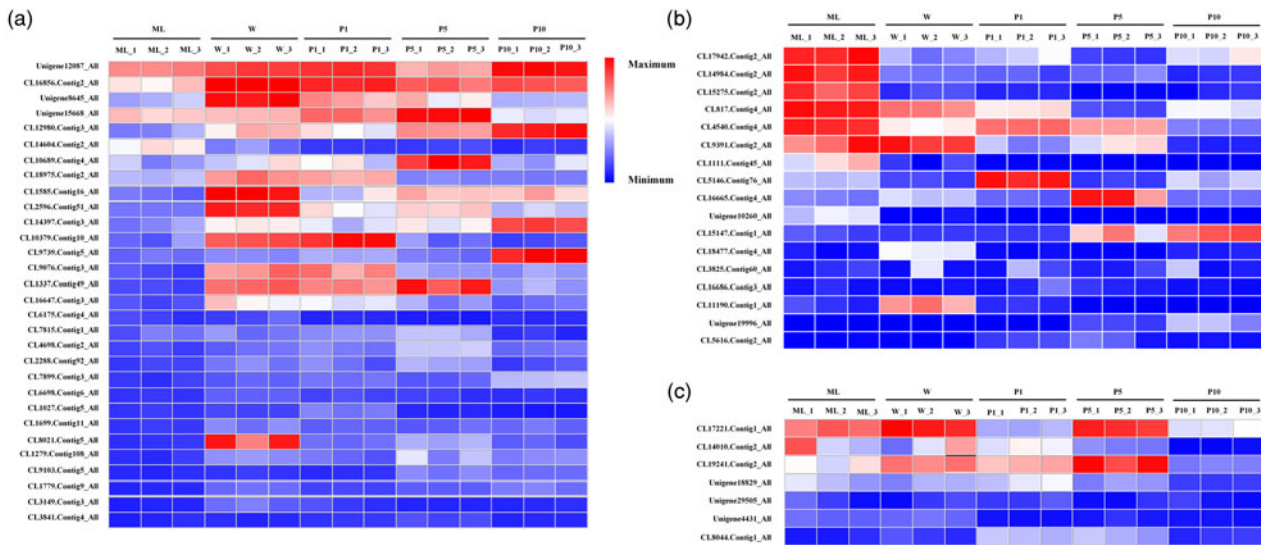


Figure 5. The heatmaps of differentially expressed genes (DEGs) were identified at different developmental stages during the prepupal-pupal transition of *M. separata* using Fragment Per Kilobase of exon model per Million mapped reads (FPKM) values. The gene IDs of cuticular proteins (a), juvenile hormone (b), and 20-hydroxyecdysone (c) are shown on the left side of the heatmaps and the developmental stages are given at the top of the heatmaps. ML, mature larvae; W, wandering; P1, P5, and P10: 1, 5, and 10 days after pupation. ML_1, ML_2, and ML_3 represent three biological replicates of ML stage. (For interpretation of the references to color in this figure legend, the reader is referred to the web version of this article.)

Expression levels of CP genes

There were 11 up-regulated and two down-regulated CP genes with a maximum $|\log_2\text{Ratio}|$ value of 3.3 (CL1279.Contig108_All) and 4.9 (CL7899.Contig3_All) in ML-vs.-W (table 2). From P1 to P5, one gene (CL9103.Contig5_All) significantly increased ($|\log_2\text{Ratio}| = 2$), and eight genes decreased (the maximum $|\log_2\text{Ratio}| = 3.8$) in expression. From W to P1 and P5 to P10, three and five genes were up-regulated, respectively (table 2).

Five genes (CL12980.Contig3_All, CL1585.Contig16_All, CL2596.Contig51_All, CL14397.Contig3_All, and CL16856.Contig2_All) were least-expressed in ML (fig. 5a). The expression levels of seven genes (unigene12087_All, CL16856.Contig2_All, unigene8645_All, CL18975.Contig2_All, CL10379.Contig10_All, CL9076.Contig3_All, and CL1337.Contig49_All) in W and P1 were higher than in other stages, while three genes (CL1585.Contig16_All, CL2596.Contig51_All, and CL1279.Contig108_All) were highly expressed in W (fig. 5a). The expression levels of three genes (Unigene15668_All, CL10689.Contig4_All, and CL1337.Contig49_All) in P5 were higher than in other stages. Three genes, including CL12980.Contig3_All, CL4397.Contig3_All, and CL9739.Contig5_All, were highly expressed in P10 while the expression level of unigene 15668_All was lower in P10 than in other stages (fig. 5a).

Expression levels of genes involved in JH biosynthesis

There were ten and six down-regulated genes from ML to W and P1 to P5, respectively, and both of them had two up-regulated genes. Compared to W, four genes were significantly increased (the maximum $|\log_2\text{Ratio}| = 3.8$) and five genes were decreased (the maximum $|\log_2\text{Ratio}| = 4.3$) in P1. There were six up-regulated and three down-regulated genes in P5-vs.-P10; of these genes, CL18477.Contig4_All and CL9391.Contig2_All showed the maximum up-regulated and down-regulated $|\log_2\text{Ratio}|$ values of 3.8 and 2.3, respectively (table 2).

Six genes (CL17942.Contig2_All, CL14984.Contig2_All, CL15275.Contig2_All, CL817.Contig4_All, CL4540.Contig4_All, and CL9391.Contig2_All) in the JH pathway were mainly expressed in ML (fig. 5b). The expression levels of CL18477.Contig4_All and CL11190.Contig1_All in W was higher than in other stages. Among five stages, CL5146.Contig76_All was highest expressed in P1 (fig. 5b). While CL17942.Contig2_All and CL817.Contig4_All were least expressed in P5, the expression level of CL16665.Contig4_All in P5 was higher than in other stages (fig. 5b). The expression levels of CL4540.Contig4_All and CL9391.Contig2_All in P10 were lower than in other stages. Meanwhile, unigene19996_All was mainly expressed in P10 (fig. 5b).

Expression levels of genes involved in 20E biosynthesis

Except for P1-vs.-P5 which has one up-regulated gene (CL17221.Contig1_All, $|\log_2\text{Ratio}| = 2.1$), there are no DEGs in the other three groups. A total of two (Unigene4431_All and CL17221.Contig1_All), one (CL14010.Contig2_All), and three (CL14010.Contig2_All, CL17221.Contig1_All, and CL19241.Contig2_All) genes were down-regulated in W-vs.-P1, P1-vs.-P5, and P5-vs.-P10, respectively (table 2). The expression of DEGs in other groups is shown in table S4. The expression levels of CL17221.Contig1_All in ML, W, and P5 were higher than in P1 and P10 (fig. 5c). Besides, CL19241.Contig2_All was mainly expressed in the P5 stage, and the expression level of CL14010.Contig2_All was lowest in P10 than in other stages (fig. 5c).

Other DEGs related to metamorphosis

In addition to the DEGs mentioned above, we also identified other 265 DEGs related to metamorphosis with a $\log_2\text{ratio}$ value ($|\log_2\text{Ratio}| \geq 10$). Among them, 28 and 11 genes were up- and down-regulated from ML to W, respectively (table S6);

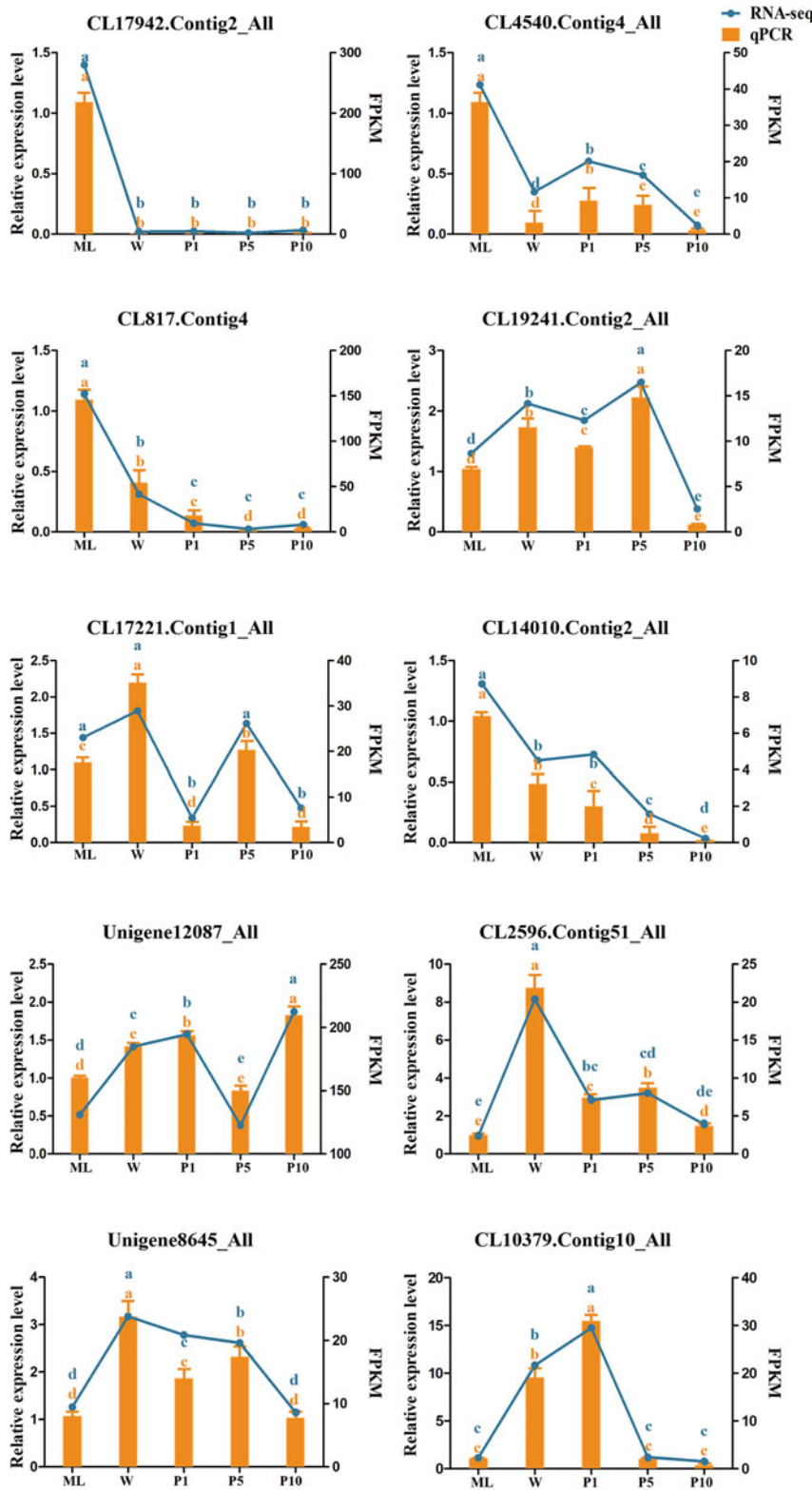


Figure 6. RT-qPCR validation of differentially expressed genes identified by RNA-Seq. Relative expression levels of ten genes, including four cuticular proteins (Unigene12087_All, CL2596.Contig51_All, Unigene8645_All, and CL10379.Contig10_All), three 20E genes (CL19241.Contig2_All, CL17221.Contig1_All, and CL14010.Contig2_All), and three JH biosynthesis genes (CL17942.Contig2_All, CL4540.Contig4_All, and CL817.Contig4_All) among different stages in *M. separata* were analyzed. Yellow columns and blue polylines indicate the relative expression levels of differentially expressed genes identified by RNA-Seq and real-time PCR quantitative (RT-qPCR), respectively. The expression was normalized to transcript levels of reference genes β -actin and GAPDH. Letters above columns and polylines represent statistically significant differences by one-way analysis of variance (ANOVA) with Duncan's test ($P < 0.05$). (For interpretation of the references to color in this figure legend, the reader is referred to the web version of this article.)

13 and four genes were up- and down-regulated from W to P1, respectively (table S7); 12 and 18 genes were up- and down-regulated from P1 to P5, respectively (table S8); 147 and 42 genes were up- and down-regulated from P5 to P10, respectively (table S9).

Validation of the expression of DEGs using qRT-PCR

Correlation analysis revealed that the relative expression levels of 10 selected CP, 20E, and JH-related genes obtained by RT-qPCR corresponded well with their FPKM values derived from RNA-seq (fig. 6).

Discussion

Insect metamorphosis is a series of changes in the external form, internal structure, physiological functions, living habits, and behavioral instincts of an insect during its development from larva to adult (Truman, 2019). The pupal stage, characteristic of holometabolous insects, is a transitional morphology between larva and adult, represents the decomposition and reconstruction of tissue and organs (Jindra, 2019). Research on these metamorphic processes might provide molecular targets that can be utilized in pest control and to confer advantages to beneficial insects.

In this study, RNA-seq was used to analyze changes in expression levels of genes during the prepupal–pupal transition in the oriental armyworm *M. separata*. A total of 74,059 unigenes were identified and annotated in the transcriptome. Using equivalent insect developmental stages such as mature larvae, wandering, and pupation stages, a total of 11,301 unigenes were annotated in *B. dorsalis* (Chen *et al.*, 2018), and 22,197 in *C. suppressalis* (Sun, 2015). These results highlight non-trivial differences in the number of genes expressed during prepupal–pupal transition across insect species. There are varied potential causes of this expression variance, such as functional differentiation of insect genes during evolution and environmental adaptation.

The epidermis covers the entire insect body surface, and not only defends against pathogen attacks and adverse environmental damage but also maintains the shape of the body and enables any required activities during development (Moussian *et al.*, 2005). A previous study has shown that 50 CP genes were significantly expressed in the prepupal–pupal transition stage of *B. mori* (Shahin *et al.*, 2016). In this study, 30 DEGs of CPs were identified, which is somewhat less than reported by Shahin *et al.* (2016). The expression patterns of CP genes in different developmental stages or tissues of insects can give clues on functionality (Andersen *et al.*, 1995). For example, the expression of CP genes from larvae to pupae in *B. mori* was significantly different (Liang *et al.*, 2010). In this study, we found that eight CP genes in W and P1 were highly expressed, while two were highly expressed in W. The expression levels of three genes in P5 were higher than in other stages, and three genes were highly expressed in P10 (fig. 5a). Togawa *et al.* (2007) found that for *A. gambiae*, five CP genes were only expressed before the pupa stage or adult molting (Togawa *et al.*, 2007). These results suggest that CP genes are involved in the formation of the epidermis during the prepupal–pupal transition in insects.

JH is produced by the corpus allatum, and its main function is regulating the growth of insects by inhibiting the action of ecdysone (Zhang *et al.*, 2018). JH plays an essential role in the growth of insect larvae, pupal metamorphosis, and adult reproduction (Raikhel *et al.*, 2005). In this study, 17 DEGs in the JH pathway were detected during the prepupal–pupal transition in *M. separata*. We found that the expression levels of six genes in the JH pathway decreased during the metamorphosis of mature larvae to pupae (fig. 5b). Our results are similar to those of Chen *et al.* (2018), who found that ten genes in the JH pathway were down-regulated during the process of larval metamorphosis in *B. dorsalis*. These results suggest that the expression of these genes in the JH pathway is to regulate deformation processes during these stages. The regulation of metamorphosis is partly the effect of JH titers (Niimi and Sakurai, 1997). Research on

insect molting and metamorphic regulation has suggested that the metamorphosis of insects occurs when the JH titer decreases continually: the concentration of JH is higher in the larval stage, and drops to a mid- or low-level during pupation, and elevates subsequently in the adult stage (Bownes and Rembold, 1987). Therefore, it needs to be determined whether the JH titer changes during the prepupal–pupal transition of *M. separata*.

Ecdysone plays a regulatory role in the growth, development, and reproduction of insects (Truman and Riddiford, 2007). Ecdysone is a steroid compound that is secreted into the hemolymph and oxidized to 20E, and which can induce insect molting (Warren *et al.*, 2002). In our study, a total of seven DEGs were highly expressed in the 20E pathway. This is similar to the result of Chen (2019) for *B. dorsalis*, who found that seven key genes of the 20E pathway were significantly overexpressed during the wandering stages. Zhao (2019) showed that the expression levels of two ecdysone receptor genes (*EcR* and *USP*) in the 6th instar larvae of *M. loreyi* was higher than that in the 5th instar. Similar results were found in our study for CL17221.Contig1_All and CL19241.Contig2_All, which is higher in W than ML (fig. 5c). We found that the expression levels of CL17221.Contig1_All and CL19241.Contig2_All was higher in P5 than in P1 or P10 (fig. 5c). Previous research showed that the expression levels of four *Halloween* genes and three ecdysone receptor genes increased first and then decreased, in male pupae of *M. loreyi* (Zhao, 2019). These studies suggest that the expression of genes encoding ecdysone may co-regulate deformation processes during the insect larval–pupal transition. The titer of 20E in insects also changes along with the developmental age, and the change of insect 20E titer is key to the regulation of larval molting, pupal metamorphosis, reproduction, and embryo development of adults (Warren *et al.*, 2002). Previous research has documented that there is a peak of 20E titer in the mid-stage of the embryo and another peak in the early stage of larval ecdysis; the higher concentration of 20E at the end of the larvae stage may be related to the initiation of transition to the pupal stage, while the higher levels of 20E in the early pupae may promote the transformation of larvae to pupae during the pre-pupal stage in *Drosophilid* (Thummel, 2001). How 20E titer changes during larval to pupal stages needs to be examined to further reveal the deformation processes of larvae–pupa in *M. separata*.

In this study, we used RNA-seq analysis in conjunction with RT-qPCR to provide a global analysis of the genes expressed from mature larvae to pupae of *M. separata*. Most genes in the prepupal–pupal transition transcriptome have been annotated according to reference information, and a large number of DEGs and pathways, especially the CPs, 20E, and JH pathways, were identified and their expression profiles characterized. These results suggest that *M. separata* prepupal–pupal transition is coordinated by hormonal regulation and is a result of a transcriptional shift of CP, 20E, and JH-associated genes (fig. 7). Collectively, the obtained transcriptome data herein not only provide a foundation for further understanding of the molecular mechanism of metamorphosis in *M. separata*, but also potentially help us to establish RNAi or CRISPR-based pest control strategies, which could operate through regulating the developmental processes of this pest.

Supplementary material. The supplementary material for this article can be found at <https://doi.org/10.1017/S0007485321000171>

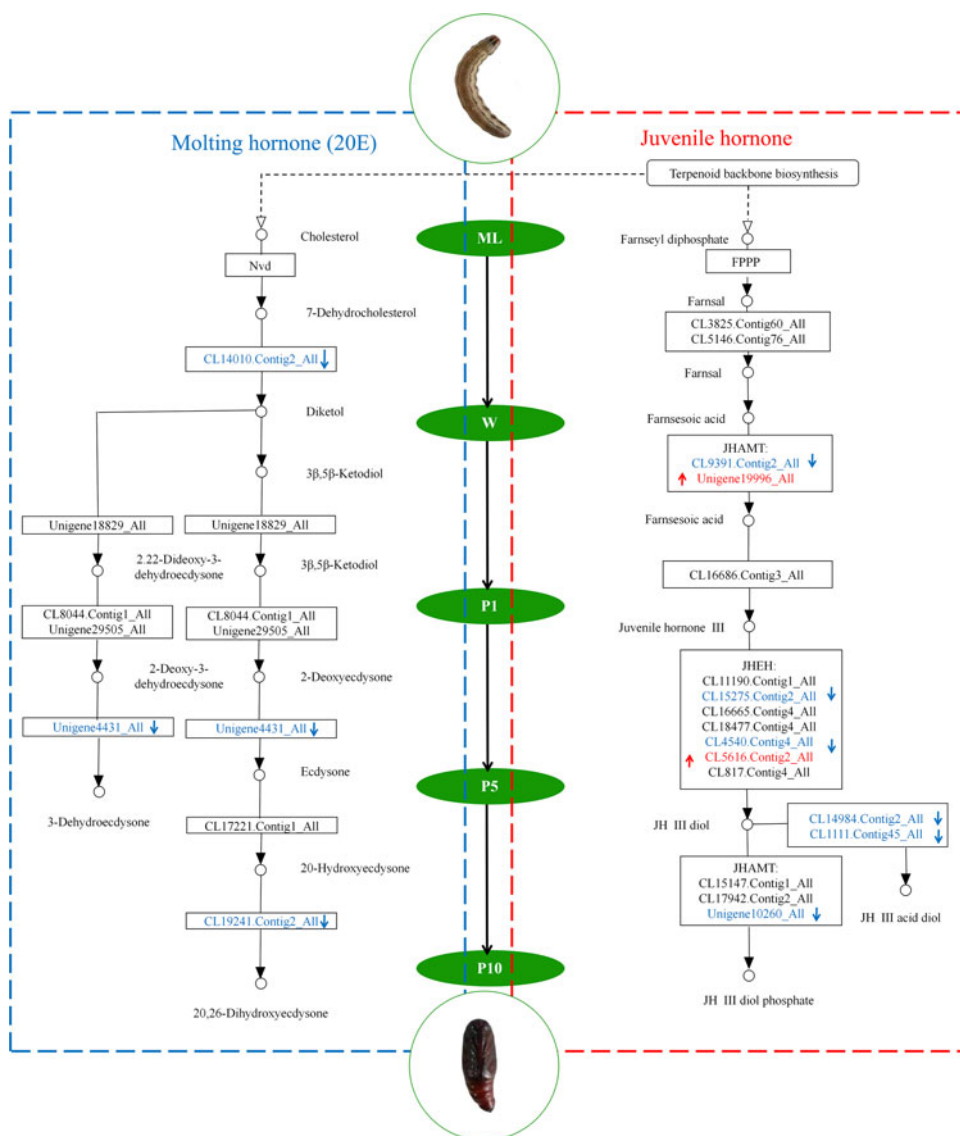


Figure 7. A proposed model of 20E and JH biosynthesis in *M. separata*. ML, mature larvae; W, wandering; P1, P5, and P10: 1, 5, and 10 days after pupation. ML_1, ML_2, and ML_3 represent three biological replicates of ML stage. (For interpretation of the references to color in this figure legend, the reader is referred to the web version of this article.) Differentially expressed genes (DEGs), which are up- and down-regulated during the prepupal–pupal transition in *M. separata* in the pathway, are indicated with red and blue font followed by red and blue arrows, respectively.

Acknowledgements. We thank Douglas Chesters (Institute of Zoology, Chinese Academy of Sciences, Beijing, China) for the language editing of this manuscript. This research was supported by the China Postdoctoral Science Foundation (2017M621160), National Major Science and Technology Projects of China (2019ZX08012004-011), the Innovative Talents Support Program of Liaoning Province (LCR2018024), and the Liaoning Revitalization Talents Program (XLYC1907097).

References

Altschul SF, Gish W, Miller W, Myers EW and Lipman DJ (1990) Basic local alignment search tool. *Journal of Molecular Biology* **215**, 403–410.

Andersen SO (2010) Insect cuticular sclerotization: a review. *Insect Biochemistry and Molecular Biology* **40**, 166–178.

Andersen SO, Hojrup P and Roepstorff P (1995) Insect cuticular proteins. *Insect Biochemistry and Molecular Biology* **25**, 153–176.

Barbora K, Vlastimil S and Marek J (2011) Common and distinct roles of juvenile hormone signaling genes in metamorphosis of holometabolous and hemimetabolous insects. *PLoS ONE* **6**, e28728.

Bownes M and Rembold H (1987) The titer of juvenile hormone during the pupal and adult stages of the life cycle of *Drosophila melanogaster*. *European Journal of Biochemistry* **164**, 709–712.

Cai MJ, Zhao WL, Jing YP, Song Q, Zhang XQ, Wang JX and Zhao XF (2016) 20-hydroxyecdysone activates Forkhead box O to promote

proteolysis during *Helicoverpa armigera* molting. *Development (Cambridge, England)* **143**, 1005–1015.

Chen EH (2019) *Identification and Functional Analysis Of Genes Coordinates With Puparium Tanning In The Oriental Fruit Fly, Bactrocera dorsalis (Hendel)* (PhD dissertation). Southwest University (in Chinese), Chongqing, China.

Chen EH, Hou QL, Dou W, Wei DD, Yue Y, Yang RL, Yu SF, De Schutter K, Smaghe G and Wang JJ (2018) RNA-seq analysis of gene expression changes during pupariation in *Bactrocera dorsalis* (Hendel) (Diptera: Tephritidae). *BMC Genomics* **19**, 693.

Cock P, Rice PM, Goto N, Heuer ML and Fields CJ (2010) The Sanger FASTQ file format for sequences with quality scores, and the Solexa/Illumina FASTQ variants. *Nucleic Acids Research* **38**, 1767–1771.

Conesa A, Gotz S, Garcia-Gomez JM, Terol J, Talon M and Robles M (2005) Blast2GO: a universal tool for annotation, visualization and analysis in functional genomics research. *Bioinformatics (Oxford, England)* **21**, 3674–3676.

Delon I and Payre F (2004) Evolution of larval morphology in flies: get in shape with shavenbaby. *Trends in Genetics* **20**, 305–313.

Dewey CN and Li B (2011) RSEM: accurate transcript quantification from RNA-Seq data with or without a reference genome. *BMC Bioinformatics* **12**, 323.

Dubrovsky EB (2004) Hormonal cross talk in insect development. *Trends in Endocrinology and Metabolism* **16**, 6–11.

Fraenkel G and Rudall KM (1940) A study of the physical and chemical properties of insect cuticle. *Proceedings of the Royal Society of London* **129**, 1–35.

- Futahashi R, Okamoto S, Kawasaki H, Zhong YS, Iwanaga M, Mita K and Fujiwara H (2008) Genome-wide identification of cuticular protein genes in the silkworm, *Bombyx mori*. *Insect Biochemistry and Molecular Biology* **38**, 1138–1146.
- Grabherr MG, Haas BJ, Yassour M, Levin JZ, Thompson SA, Amit I, Adiconis X, Fan L, Raychowdhury R, Zeng QD, Chen ZH, Mauceli E, Hacohen N, Gnirke A, Rhind N, Palma FD, Birren BW, Nusbaum C, Lindblad-Toh K, Friedman N and Regev A (2011) Trinity: reconstructing a full-length transcriptome without a genome from RNA-Seq data. *Nature Biotechnology* **29**, 644–652.
- Gu J, Huang LX, Gong YJ, Zheng SC, Liu L, Huang LH and Feng QL (2013) De novo characterization of transcriptome and gene expression dynamics in epidermis during the larval-pupal metamorphosis of common cutworm. *Insect Biochemistry and Molecular Biology* **43**, 794–808.
- Guan X, Middlebrooks BW, Alexander S and Wasserman SA (2006) Mutation of *TweedleD*, a member of an unconventional cuticle protein family, alters body shape in *Drosophila*. *PNAS* **103**, 16794–16799.
- Iseli C, Jongeneel CV and Bucher P (1999) ESTScan: a program for detecting, evaluating, and reconstructing potential coding regions in EST sequences. *International Conference on Intelligent Systems for Molecular Biology* **99**, 138–148.
- Jia QQ, Liu SN, Wen D, Cheng YX, William B, Wang J and Li S (2017) Juvenile hormone and 20-hydroxyecdysone coordinately control the developmental timing of matrix metalloproteinase-induced fat body cell dissociation. *Journal of Biological Chemistry* **292**, 21504–21516.
- Jiang YY, Li CG, Zeng J and Liu J (2014) Population dynamics of the armyworm in China: a review of the past 60 years' research. *Chinese Journal of Applied Entomology* **51**, 890–898 (in Chinese).
- Jindra M (2019) Where did the pupa come from? The timing of juvenile hormone signalling supports homology between stages of hemimetabolous and holometabolous insects. *Philosophical Transactions of the Royal Society B Biological Sciences* **374**, 20190064.
- Jindra M, Palli SR and Riddiford LM (2013) The juvenile hormone signaling pathway in insect development. *Annual Review of Entomology* **58**, 181–204.
- Li HB, Dai CG, Zhang CR, He YF, Ran HY and Chen SH (2018) Screening potential reference genes for quantitative real-time PCR analysis in the oriental armyworm, *Mythimna separata*. *PLoS ONE* **13**, e0195096.
- Li MM, Li BL, Jiang SX, Zhao YW, Xu XL and Wu JX (2019a) Microsatellite-based analysis of genetic structure and gene flow of *Mythimna separata* (Walker) (Lepidoptera: Noctuidae) in China. *Ecology and Evolution* **9**, 13426–13437.
- Li XR, Li Y, Wang W, He N, Tan XL and Yang XQ (2019b) LC50 of lambda-cyhalothrin stimulates reproduction on the moth *Mythimna separata* (Walker). *Pesticide Biochemistry and Physiology* **153**, 47–54.
- Liang JB, Zhang L, Xiang ZH and He NJ (2010) Expression profile of cuticular protein genes of silkworm, *Bombyx mori*. *BMC Genomics* **11**, 173.
- Liu X, Dai FY, Guo EE, Li K, Ma L, Tian L, Cao Y, Zhang GZ, Palli SR and Li S (2015) 20-Hydroxyecdysone (20E) primary response gene E93 modulates 20E signaling to promote Bombyx larval-pupal metamorphosis. *Journal of Biological Chemistry* **290**, 27370–27383.
- Liu PC, Fu XN and Zhu JS (2018) Juvenile hormone-regulated alternative splicing of the taiman gene primes the ecdysteroid response in adult mosquitoes. *PNAS* **115**, 7738–7747.
- Livak KJ and Schmittgen TD (2001) Analysis of relative gene expression data using real-time quantitative PCR and the $2^{-\Delta\Delta CT}$ method. *Methods (San Diego, California)* **25**, 402–408.
- Love MI, Huber W and Anders S (2014) Moderated estimation of fold change and dispersion for RNA-seq data with DESeq2. *Genome Biology* **15**, 550.
- Moussian B, Schwarz H, Bartoszewski S and Nüsslein-Volhard C (2005) Involvement of chitin in exoskeleton morphogenesis in *Drosophila melanogaster*. *Journal of Morphology* **264**, 117–130.
- Niimi S and Sakurai S (1997) Development changes in juvenile hormone and juvenile hormone acid titers in the hemolymph and *in-vitro* juvenile hormone synthesis by corpora allata of the silkworm, *Bombyx mori*. *Journal Insect Physiology* **43**, 875–884.
- Nijhout HF and Callier V (2015) Developmental mechanisms of body size and wing-body scaling in insects. *Annual Review of Entomology* **60**, 141–156.
- Pertea G, Huang X, Liang F, Antonescu V, Sultana R, Karamycheva S, Lee Y, White J, Cheung F, Parvizi B, Tsai J and Quackenbush J (2003) TIGR Gene Indices clustering tools (TGICL): a software system for fast clustering of large EST datasets. *Bioinformatics (Oxford, England)* **19**, 651–652.
- Qu Z, Bendena WG, Tobe SS and Hui JHL (2018) Juvenile hormone and sesquiterpenoids in arthropods: biosynthesis, signaling, and role of MicroRNA. *Journal of Steroid Biochemistry and Molecular Biology* **184**, 69–76.
- Raikhel AS, Brown MR and Belles X (2005) Hormonal control of reproductive processes. *Comprehensive Molecular Insect Science* **3**, 433–491.
- Shahin R, Iwanaga M and Kawasaki H (2016) Cuticular protein and transcription factor genes expressed during prepupal-pupal transition and by ecdysone pulse treatment in wing discs of *Bombyx mori*. *Insect Molecular Biology* **25**, 138–152.
- Sharma HC, Sullivan DJ and Bhatnagar VS (2002) Population dynamics and natural mortality factors of the oriental armyworm, *Mythimna separata* (Lepidoptera: Noctuidae), in South-Central India. *Crop Protection* **21**, 721–732.
- Sugahara R, Tanaka S and Shiotsuki T (2017) RNAi-mediated knockdown of SPOOK reduces ecdysteroid titers and causes precocious metamorphosis in the desert locust *Schistocerca gregaria*. *Developmental Biology* **429**, 71–80.
- Sun Y (2015) *Functional Analysis of Protein Coding Gene and miRNA in Pupa and Pupa Development in Chilo Suppressalis* (PhD dissertation). Nanjing Agricultural University (in Chinese), Nanjing, China.
- Thummel CS (2001) Molecular mechanisms of developmental timing in *C. elegans* and *Drosophila*. *Developmental Cell* **1**, 453–465.
- Togawa T, Dunn WA, Emmons AC and Willis JH (2007) Cpf and cpfl, two related gene families encoding cuticular proteins of *Anopheles gambiae* and other insects. *Insect Biochemistry and Molecular Biology* **37**, 675–688.
- Truman JM (2019) The evolution of insect metamorphosis. *Current Biology* **29**, 1252–1268.
- Truman JW and Riddiford LM (1999) The origins of insect metamorphosis. *Nature* **401**, 447–452.
- Truman JW and Riddiford LM (2002) Endocrine insights into the evolution of metamorphosis in insects. *Annual Review of Entomology* **47**, 467–500.
- Truman JW and Riddiford LM (2007) The morphostatic actions of juvenile hormone. *Insect Biochemistry and Molecular Biology* **37**, 761–770.
- Wang GP, Zhang QW, Ye ZH and Luo LZ (2006) The role of nectar plants in severe outbreaks of armyworm *Mythimna separata* (Lepidoptera: Noctuidae) in China. *Bulletin of Entomological Research* **96**, 445–455.
- Warren JT, Petryk A, Marques G, Jarcho M, Parvy JP, Dauphin-Villemant C, O'Connor MB and Gilbert LI (2002) Molecular and biochemical characterization of two P450 enzymes in the ecdysteroidogenic pathway of *Drosophila melanogaster*. *PNAS* **99**, 11043–11048.
- Willis JH (2010) Structural cuticular proteins from arthropods: annotation, nomenclature, and sequence characteristics in genomics era. *Insect Biochemistry and Molecular Biology* **40**, 189–204.
- Ye ZH (1993) *Major Agricultural Biological Disasters and Disaster Reduction Measures in China*. National Science and Technology Commission National Major Natural Disasters Comprehensive Research Group. Discussion on Major Natural Disasters and Disaster Reduction Measures in China. Beijing: Science Press, pp. 549–602 (in Chinese).
- Zhai Y, Zhang Z, Gao H, Chen H, Sun M, Zhang W, Yu Y and Zheng L (2017) Hormone signaling regulates nymphal diapause in *Laodelphax striatellus* (Hemiptera: Delphacidae). *Scientific Reports* **7**, 13370.
- Zhang X and Zheng S (2017) 20-hydroxyecdysone enhances the expression of the chitinase 5 via broad-complex zinc-finger 4 during metamorphosis in silkworm, *Bombyx mori*. *Insect Molecular Biology* **26**, 243–253.
- Zhang Y, Huang J, Zhou B, Zhang C, Liu W, Miao X and Huang Y (2009) Up-regulation of lysozyme gene expression during metamorphosis and immune challenge of the cotton bollworm, *Helicoverpa armigera*. *Archives of Insect Biochemistry and Physiology* **70**, 18–29.
- Zhang Z, Liu X, Shiotsuki T, Wang Z, Xu X, Huang Y, Li MW, Li K and Tan AJ (2017) Depletion of juvenile hormone esterase extends larval growth in *Bombyx mori*. *Insect Biochemistry and Molecular Biology* **81**, 72–79.
- Zhang T, Song W, Li Z, Qian W, Wei L, Yang Y, Wang WN, Zhou X, Meng M, Peng J, Xia QY, Perrimon N and Cheng DJ (2018) Krüppel homolog 1 represses insect ecdysone biosynthesis by directly inhibiting the transcription of steroidogenic enzymes. *PNAS* **115**, 3960–3965.
- Zhao YW (2019) *Analysis of Expression Pattern of Ecdysone Synthesis and Related Receptor Genes of Mythimna loreyi* (Master dissertation). Northwest A&F University (in Chinese), Yangling, China.